J Appl Electrochem (2011) 41:321–336
DOI 10.1007/s10800-010-0242-3

ORIGINAL PAPER

Novel electrochemical measurements on direct electro-deoxidation of solid TiO_2 and ZrO_2 in molten calcium chloride medium

K. S. Mohandas · D. J. Fray

Received: 28 August 2010 / Accepted: 31 October 2010 / Published online: 14 December 2010

Abstract A solid metal oxide cathode undergoes significant chemical changes during the molten salt electro-deoxidation process. The changes in the chemical composition lead to changes in the electrical resistivity and potential of the electrode. Two novel electrochemical techniques, based on these two parameters, have been employed to study the electro-deoxidation of solid TiO_2 and ZrO_2 in molten calcium chloride at 900 °C. The in situ resistance measurements carried out by the IR drop method conclusively proved that TiO_2 electrode remains highly conducting throughout the electro-deoxidation process and hence is amenable for reduction. The ZrO_2 electrode, on the other hand, developed very high resistance midway in the electro-deoxidation, and could not be reduced completely. The resistance measurements give strong indication that the electron-transfer reactions taking place at the cathode determine the rate and efficiency of the electro-deoxidation process to a great extent. The low-current galvanostatic electro-deoxidation of TiO_2 electrodes, in conjunction with a graphite pseudo reference electrode to monitor the half cell potentials, showed that the metal oxide passes through two stages during the electrolysis; a high current, low resistant stage 1, where Ca^{2+} ions are inserted to the metal oxide cathode to produce different intermediate compounds and stage 2 where electro-deoxidation of the cathode take place continuously. Removal of oxygen, from the cathode, in stage 1 of the electro-deoxidation is considered to be insignificant. The anodic and cathodic voltages in this stage remained more or less stable at ~ 1.4 V and ~ -1 V, respectively. When the oxygen ions in the melt were depleted at the end of this stage, both the anode and cathode potentials were increased in the anodic direction and this behaviour suggested that the graphite pseudo reference electrode was changed from a C/CO electrode in stage 1 to a Ca^{2+}/Ca electrode in stage 2.

Keywords FFC Cambridge Process · Zirconium dioxide · Titanium dioxide · Electro-deoxidation · Molten salt · IR drop · Resistance measurement

K. S. Mohandas · D. J. Fray (✉)
Department of Materials Science & Metallurgy, University of Cambridge, Cambridge CB2 3QZ, UK
e-mail: djf25@cam.ac.uk

Present Address:
K. S. Mohandas
Fuel Chemistry Division, Chemistry Group, Indira Gandhi Centre for Atomic Research, Kalpakkam 603 102, Tamil Nadu, India
e-mail: ksmd@igcar.gov.in

1 Introduction

Production of metals from its compounds has been an important area of metallurgical activity across the world for many decades. Both chemical and electrochemical methods have been employed for production of metals. Recently, a novel electrochemical method called 'FFC Cambridge Process' was added to these technologies for production of metals and alloys from their oxides. In this unique process, a solid oxide is directly converted to the respective metal by electro-deoxidation in a molten calcium chloride bath containing small amounts of calcium oxide at ~ 900 °C [1–5]. The solid metal oxide itself serves as the cathode, and a compacted graphite rod is generally used as the anode. When electrons are passed into the metal oxide from an external power source, the oxygen present in the metal oxide combines with the electrons and leaves the

cathode as oxygen ions which discharge at the graphite anode and liberate CO/CO_2 gas. The process was demonstrated for production of many metals [6–12], semi-metal [13, 14] and alloys [15–19]. We have also investigated the electro-deoxidation behaviour of zirconium dioxide in the process [20].

In conventional electrochemical process for metal production, the metal compound is directly electrolysed from an electrolyte medium, in which it is dissolved as ions. Under the influence of the applied potential, the cations and anions are transported to the respective electrodes and discharge to produce the metal/non-metal component of the compound. However, in the new process, the metal oxide is not dissolved in the electrolyte and exists as a solid block in contact with the molten electrolyte in the electrochemical cell. This unique configuration of the electrode makes the new process very different from the conventional electrochemical processes, and it calls for novel cell designs, new methods of analysis and monitoring for the electrolytic process. One such novel technique can be based on the electrical resistivity of the cathode, as it varies from that of an insulator at the start to a metal at the end of the electro-deoxidation process.

Many studies on the direct electro-deoxidation of different metal oxides have shown that, in the initial stage of electrolysis, the metal oxides react cathodically with the calcium ions in molten calcium chloride or the calcium oxide dissolved in it to produce low valent metal oxides as well as ternary compounds of the type, Ca_x–M_y–O_z, which are subsequently deoxidized under the applied potential conditions to produce the metal. This means that the chemical composition of the electrode as well as the electrolyte is undergoing continuous change during the electro-deoxidation process. For example, electro-deoxidation of solid TiO_2 is reported to proceed through formation/decomposition of different sub-oxides with decreasing valences, such as Ti_4O_7, Ti_3O_5, Ti_2O_3 and TiO in conjunction with calcium containing ternary compounds, such as $CaTiO_3$ and $CaTi_2O_4$ [6, 7]. Our investigation on the electro-deoxidation of zirconium dioxide showed that a stable intermediate compound, $CaZrO_3$, is formed during the reduction process, which undergoes electro-deoxidation in the later stages of electrolysis to yield zirconium metal [20]. Good electrical conductivity of the electrode, during the entire period of electrolysis is a pre-requisite for better efficiency of the electro-deoxidation process or for that matter any electrochemical process. As the electrical conductivity of the cathode in the electro-deoxidation cell is related to its chemical composition, the measurement of electrical resistance of the cathode during the course of electro-deoxidation, will be very important for developing a better understanding of the fundamentals of the electrochemical process. The general practice is to withdraw partially electro-deoxidized samples from the reactor during the course of electro-deoxidation and subject the samples to analysis after mandatory cooling/cleaning steps. This is a very cumbersome procedure. Also some information on the intermediate compounds formed during electrolysis may be lost with this kind of an analysis, as the solid sample needs to be cooled to room temperature and thoroughly cleaned from the adhering salt before any analysis could be done. Such issues can be circumvented to a good extent, if the information can be obtained by in situ electrochemical measurements on the cell.

Mohandas et al. applied IR drop measurements combined with low-current galvanostatic polarization techniques and cyclic voltammetry to study the fundamentals of solid-state electrode reactions taking place in molten salt electrolytic cells [21–26]. These novel techniques were successfully employed to distinguish between the electrochemical adsorption and intercalation of chloride/chloroaluminate ions taking place on a graphite anode in molten sodium chloroaluminate medium [22] and to measure, electrochemically, the standard Gibbs energy of formation of solid sodium chloride at its sub-melting temperatures ($\sim$523 K) [23, 24]. It was proved in these studies that electrochemical techniques, could be fine tuned to study the chemical composition of an electrolyte medium or an electrode and also to obtain the electrode resistances and polarization over voltages of an electrochemical cell. In this article, we report the investigations carried out on the electro-deoxidation of both TiO_2 and ZrO_2 electrodes using the novel electrochemical techniques.

2 Experimental details

2.1 Electrode preparation

Both TiO_2 and ZrO_2 electrodes were prepared from the powders (average particle size 1–2 μm) supplied by Alfa-Aesar. The oxide precursor powders were mixed with 1% by mass of a mixture of the binder, PVB/PVA (Poly vinyl butyral-*co*-vinyl alcohol-*co*-vinyl acetate-80% by weight vinyl butyral, Aldrich Chemicals) and 0.5% by mass of the plasticizer, polyethylene glycol (average molecular mass 200, Aldrich Chemicals) in a mortar. The mixture was wet milled with isopropyl alcohol and the slurry was partially dried in air. It was further dried in an oven at 80 °C, until all the alcohol had evaporated. The dry mass was thoroughly powdered and uniaxially pressed in a hydraulic press with a uniaxial pressure in the range of 5–25 MPa (2–3 T) to make pellets of 13- and 20-mm diameter. The thickness and weight of the pellets varied from 2 to 5 mm and from 1.5 to 4.0 g, respectively. The pellets were sintered at 1000 and 1250 °C for 3 or 5 h in a programmable

electrical furnace with a heating rate of 5 °C/min. The porosities of the pellets were measured using the Archimedes method in water. The open porosity of the ZrO_2 pellets, sintered at 1000 and 1250 °C, were 33.1 and 22.5%, respectively. The corresponding values for TiO_2 were 40.5 and 6.9%.

2.5-mm diameter holes were drilled at the centre of the sintered pellets with the help of a hand drill and nickel current collector wires (2 mm dia. × 600 mm long) were connected to the pellets by insertion through the holes. Compacted graphite rods (10 mm dia. × 100 mm long) threaded to stainless steel rods (3 mm dia. × 600 mm long) were used as anodes as well as pseudo-reference electrodes. The graphite rods were degassed at 350 °C under vacuum and stored in an oven at 150 °C before use in the experiments.

2.2 Cell and electrical connections

A vertical tubular reactor vessel made of Inconel 600 (125 mm i.d × 625 mm ht.) and with a 6-mm-thick flange welded at its open end was used in the experiments. Holes were drilled on the top lid of the reactor vessel, through which the electrodes were introduced to the reactor. Silicone rubber bungs and Viton O-rings were used to make the reactor leak tight. Anhydrous calcium chloride (Fluka), contained in alumina crucibles, was used as the electrolyte and was dried, under vacuum, at 200 °C for 48–72 h and stored in airtight bottles before use in the experiments. The salt was heated slowly up to 750 °C in the experimental vessel and then to the experimental temperature of 900 °C. The heating programme involved heating of the salt from room temperature to 300 °C at 40 °C/min, dwelling for 2 h, heating to 750 °C at 50 °C/min, dwelling for 1 h, and heating to the operation temperature of 900 °C at 60 °C/min. The calcium chloride, dried as above, normally contained about 0.1 mol% CaO, but higher concentrations are also possible depending on the quality of the salt and its drying procedure. The experiments were conducted under an inert gas by continuously purging the reactor with argon gas. The argon gas, before being admitted into the reactor, was made moisture-free by passing it through self-indicating calcium sulphate (Drierite 8 mesh with indicator, Aldrich). The reactor outlet was connected to a bottle containing concentrated H_2SO_4, which insulated the reactor environment from ambient atmosphere and also served as a physical indicator of the flow of argon gas through the reactor. An argon gas flow rate of 75–125 lpm was maintained through the reactor during the experiments.

The sintered oxide pellets were introduced to the reactor with the help of 2-mm diameter nickel wire, which passed through the silicone rubber bungs which were inserted into the top lid of the reactor vessel. The graphite anode, 10-mm dia., threaded to 3-mm-dia. stainless steel rod, was similarly introduced to the reactor vessel. Two such graphite anodes were used when two oxide electrodes were simultaneously electrolysed. A third graphite electrode was used as a pseudo-reference electrode. This electrode was connected to the oxide electrode (cathode) through a voltmeter with an aim to monitor the cathodic potentials during electrolysis. Schwandt and Fray have demonstrated that a compacted graphite rod could be used as a pseudo-reference electrode in molten calcium chloride–calcium oxide system [12]. Often, it was necessary to compare the electro-deoxidation behaviour of two different kinds of oxides (e.g. TiO_2 and ZrO_2) or two electrodes of the same oxide with a difference in their physical parameters (e.g. porosity) or electrolysis of two identical electrodes under different electro-deoxidation conditions (constant voltage/constant current modes). For this study, two oxide electrodes were simultaneously electro-deoxidized in the same electrolyte, but with two independent anodes and DC power supply units. This 'two-in-one' cell arrangement enabled electro-deoxidation of the two electrodes independently, but at the same time maintaining all other parameters, except the one under study, identical for both the electrodes. Pellets of identical mass and close physical dimensions were only used in such experiments to avoid any contribution to the measured resistance from the difference in the mass and dimension of the pellets. In a typical two-in-one cell with one independent reference electrode for each cell, there will be four voltage measurement channels (two channels for overall cell voltage and two channels for the reference cell voltages) and two current measurement channels. Often the data were acquired continuously throughout the duration of electro-deoxidation, which varied from a few hours to over 100 h. The multiple task of voltage and current measurements were carried out using an Agilent 34970A data acquisition/switch unit with a 20-channel multiplexer unit attached to it.

The anodic process of the electro-deoxidation cell is the discharge of O^{2-} ions, and hence the use of two anodes in the two-in-one cell may look unnecessary, especially when the applied voltages of the two cells are same. However, a finer analysis will show that it is not the case. When two oxide cathodes with different physical/chemical characteristics are used, the cathodic deoxidation behaviour and, hence the resulting currents, will be different for the two electrodes. Also, the resistances of the two cathodes will be different. The situation will result in different IR drops for the two cells, which in turn makes the effective potentials of the two anodes different, for the same applied voltage. Further, the resistance of the individual cells and their half-cells can be measured, only if the two cells are independent.

The current and voltage measurements were made in the DC four-contact configuration [21, 27], in which the voltage measuring leads were separated from the current

carrying leads. In this mode of connection, the DC power supply and the experimental cell are connected in series, and the electrode voltage is measured with an independent voltmeter connected parallel to the cell, at the closest point of the electrochemical cell. The schematic of a typical two-in-one electrolysis cell and its electrical connections is given in Fig. 1. The DC four-contact configuration is depicted in Fig. 2. The electrical circuit diagram of the two-in-one electro-deoxidation cell is given in Fig. 3.

2.3 Electro-deoxidation conditions

Electro-deoxidation was carried out in both constant voltage and constant current modes. The constant voltage experiments were carried out at the applied voltages of 3.0–3.1 V, across the electrodes, and constant current experiments with currents in the range of 50–100 mA. In the case of constant voltage electrolysis, the completion of the electro-deoxidation reaction was inferred when the current decreased to lower values close to background levels and stabilized with time. For constant current electrolysis, the end reaction can be considered as the decomposition of the molten electrolyte, and hence the potential window of the DC power supply was kept at 3.3 V, little above the decomposition potential of calcium chloride electrolyte (~3.2 V). However, owing to IR and polarization losses, the actual potential difference between the anode and cathode will be less than 3.3 V. Two independent power supply units

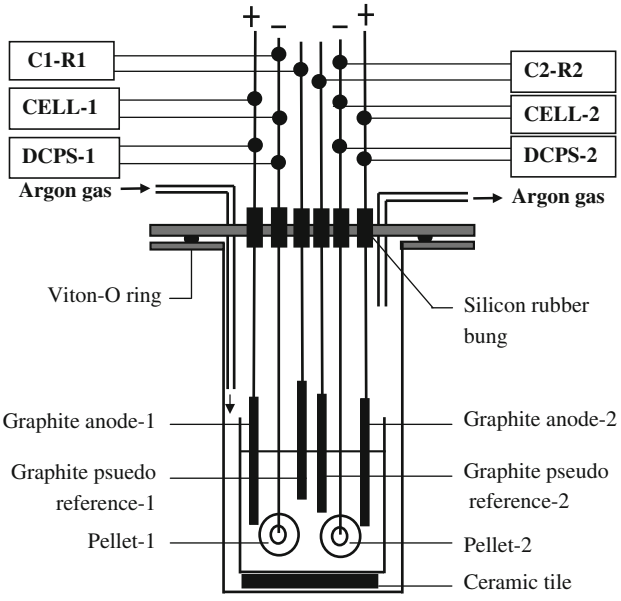

Fig. 1 Schematic of the cell for simultaneous electrolysis of two oxide pellet electrodes (two-in-one cell) in molten calcium chloride. The two pellets are the cathodes of the two independent cells. The electrical connections are given in the DC four-contact configuration (*DCPS* DC power supply, *CELL* the overall cell voltage, *C–R* cathode versus reference)

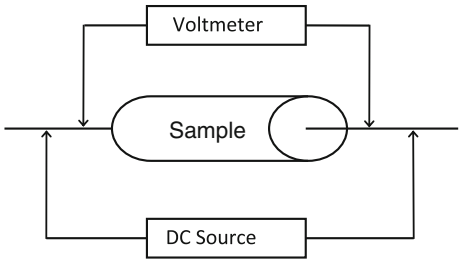

Fig. 2 Schematic of the DC four-contact configuration. The voltmeter leads need to be connected as closely as possible to the cell (sample) and inside the current leads so that the IR drops of the sample and the lead wires up to the point of the voltmeter connection can be obtained during the IR drop measurement

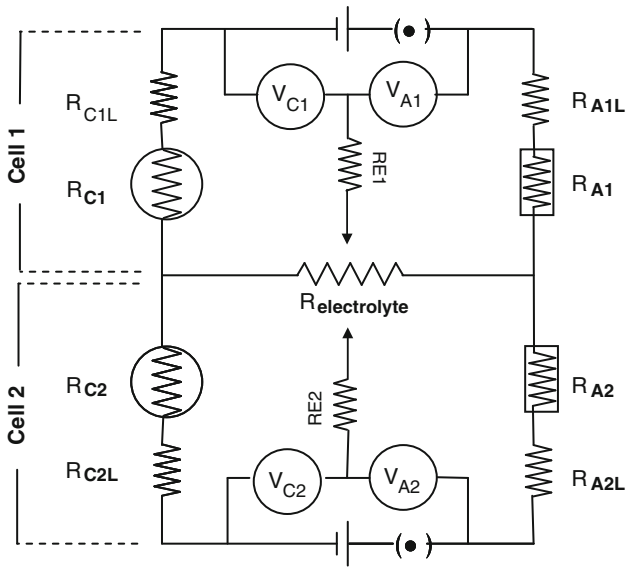

Fig. 3 The circuit diagram of a two-in-one cell for simultaneous electro-deoxidation of two cathodes in the same electrolyte. Except the electrolyte, the two cells (Cell 1 and Cell 2) are independent. The subscripts 'C' and 'A' denote the cathode and anode of the two cells, respectively and (V_C) and (V_A), the cathode and anode half cell potentials, respectively. RE1 and RE2 represent the two graphite pseudo-reference electrodes used in the half cell potential measurements of Cell 1 and Cell 2, respectively. R_L refers to the lead wire resistance of the respective electrodes

(Thurbly Thander PL154 with 15 V and 4 A capacity) were used. The process temperature was maintained at 900 °C using an electrical furnace and a Eurotherm temperature controller in conjunction with a K-type thermocouple.

2.4 Analysis and characterization

After electro-deoxidation, the pellets were lifted out of the melt and positioned in the upper part of the reactor and allowed to cool to room temperature, under a flowing argon gas atmosphere. The pellets were washed with water to remove the adhering frozen calcium chloride and cleaned

further by vacuum impregnation in 1 N HCl solution for about 12 h. The pellets were again vacuum-impregnated with water. The clean pellets were rinsed with acetone and dried in air at 70 °C.

The cleaned pellets were characterized using X-ray diffraction analysis (PW 1710, PHILIPS) with copper K_α radiation. A Scanning Electron Microscope (JSM 5800-LV, JEOL) was used to obtain the morphology of the pellets before and after electrolysis. Chemical analysis of the samples was carried out with a Noran Voyager EDS system attached to the SEM.

2.5 Measurement techniques and conditions

2.5.1 IR drop method of resistance measurement

The DC four-contact configuration of the electrical connections shown in Fig. 1 enables current interruption (CI) to be performed on the electrolytic cell during both constant current and constant voltage electrolyses. The method of current interruption, as employed in this study is rather simple; just manually break the current circuit by switching off the DC power supply and record the instantaneous back emf of the resultant galvanic cell. The instantaneous voltage difference between the electrolytic and galvanic cell is IR. The IR, when divided by the current at the instance of CI gives R, the resistance of the cell. The relationship can be expressed as,

$$E_{\text{cell}} = E_{\text{rev}} + \text{IR} + \eta_{\text{a+c}} \text{ (Electrolytic cell)}$$
$$\downarrow \text{CI}$$
$$E_{\text{cell}} = E_{\text{rev}} + \eta_{\text{a+c}} \text{ (Galvanic cell)}$$

where E_{cell} and E_{rev} are, respectively, the applied voltage of the electrolytic cell and reversible thermodynamic potential of the electrochemical reaction, and $\eta_{\text{a+c}}$, the combined electrode polarization of the anode and cathode. The cell resistance, R is the sum total of the resistances of the individual components of the cell, viz. the electrolyte melt, the electrodes and the lead wires. In the case of an electro-deoxidation cell, the resistance of the cathode and the molten electrolyte will change during the course of the electro-deoxidation whereas that of the lead wires and the anode will remain constant at the constant temperature of the cell. Hence, the resistance of the cell measured at different times during the course of the experiment will be the sum of the resistances of the cathode and the electrolyte. When the electrolyte resistance is negligible compared to the cathode resistance, the cell resistance can be approximated to the cathode resistance. The electrolyte resistance of an electro-deoxidation cell with graphite anode may change during the process, and hence it may be difficult to obtain the cathode resistance in the above method, especially towards the later stages of electro-deoxidation. However, when two cathodes are simultaneously electro-deoxidized in the same melt, all the resistive components except the cathodes become identical for the two cells, and, hence, the change in the cell resistance between the two cells can be attributed to the resistance changes occurring at the two oxide cathodes. As one of the electrodes in the electro-deoxidation cell is a gas-evolving electrode [$C/CO_2/CO$], the back emf of the cell should be measured at the instance of current interruption or else the anodic product gases would diffuse away from the electrode to give rise to erroneous galvanic cell potential values. It will be a good practice to take two or three measurements in such situations after allowing sufficient time in between the measurements for the cell to revert to its original cell voltage. When electro-deoxidation is carried out in the constant current mode (galvanostatic polarization) at very low current densities, the IR drop measurements as explained above could give valuable information on the fundamental aspects of the electro-deoxidation, as will be discussed later in Sect. 3.2.

The drop in the IR voltage during current interruption will be shown as vertical lines in the voltage–time profile. During current interruption, the electrode reactions are momentarily reversed. When such disturbances take place in a solid matrix, it takes a while for the cell to stabilize and revert to its original electrolytic cell potential when the current circuit is re-established. This time lag might lead to some discontinuity in the voltage–time plots, as can be noticed in the in V–t plots given in Fig. 8.

The typical behaviour of cell voltage during current interruption in an ideal electrolytic cell and its reversal on re-establishment of the current circuit is shown in Fig. 4. It can be noticed that the current-dependent IR part vanishes instantaneously from the cell voltage on current interruption, whereas the time-dependent polarization voltage

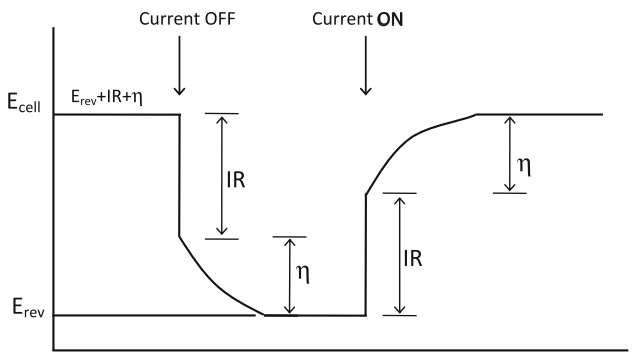

Fig. 4 Schematic of the potential behaviour of an ideal electrolytic cell on current interruption. The current-induced IR drop vanishes instantaneously on current interruption, whereas the time-dependent polarization part decreases (depolarization) slowly to the stable galvanic cell potential. The opposite of the potential behaviour happens when the cell current is restored

decreases exponentially with time. A reversal of the trend happens on re-establishment of the current circuit.

The cell resistance measured by the IR drop method, as explained above, includes the resistance of the electrode, electrolyte and lead wires. The procedure can be extended to measure the resistance of a single electrode of an electrochemical cell. In this measurement, the working electrode of the electrolytic cell is electrically connected, through a voltmeter, to a suitable reference electrode in the cell. When current '*I*' was passed through the electrolytic cell circuit, the reference cell voltage was observed to increase by IR, the *R* being the sum of the resistances of the working electrode, the lead wire of the working electrode up to the point of voltage measurement and the electrolyte column between the working and the reference electrodes. If the combined resistance of the lead wire and the electrolyte is insignificant compared to the resistance of the working electrode, then the measured resistance can be approximated to that of the working electrode. When comparing the single electrode potentials of a two-in-one cell, all the resistive components except the one under question, will cancel out as explained before. This method was used to obtain the resistance/IR drop of the anode and cathode in the galvanostatic electro-deoxidation experiment discussed in Sect. 3.2.

2.5.2 *Galvanostatic polarization*

The controlled current technique was used to obtain qualitative and quantitative information of the electro-deoxidation process. The charge passed through an electrolytic cell at constant current '*I*' is $Q\ (Ah) = It$ where '*t*' is the duration of electro-deoxidation in hours. The cell voltage will remain more or less steady if sufficient electroactive species are available to sustain the constant current at that potential. When the ionic species that correspond to the particular decomposition reaction are exhausted in the electrolyte, the cell voltage will increase automatically to a higher value so that the constant current is sustained by a decomposition reaction requiring higher energy. When the applied current density is very small, the voltage step from one electrolytic decomposition reaction to another becomes distinct, and hence it becomes possible to identify the different decomposition reactions in the electrolyte medium. With the use of a reference electrode in the cell, information on the electrochemical reactions taking place on individual electrode could be obtained. In the case of a molten salt electrochemical cell operating at elevated temperatures, the electrode processes at very low current densities can be considered to take place close to thermodynamic equilibrium conditions. This can be used for obtaining fundamental thermodynamic and kinetic information on the electrode processes [22–24]. Such measurements are not possible on a cell operating at constant applied potentials as the cell reactions are dictated by the impressed potential in that case.

While the technique could be employed very successfully with a conventional electrochemical cell, where the ions are free to move in a liquid electrolyte medium, it may not be possible to apply the technique with equal measure of success to the direct electro-deoxidation reactions as the complex electrochemical reactions take place in the solid state with formation and decomposition of different solid phases.

The potentials of the chemical reactions given in this article are referred to Ca/Ca^{2+} equilibrium ($Ca/Ca^{2+} = 0$ at 900 °C) with the reactants and products existing in their standard states. We have followed the reaction scheme and the potentials proposed by Schwandt and Fray [6] for the discussions on the electro-deoxidation of TiO_2.

3 Results and discussions

3.1 Electrode resistance and reaction pathways

In a typical electro-deoxidation cell with molten calcium chloride electrolyte containing dissolved CaO, the ionic current will predominantly be carried by O^{2-} ions generated at the oxide cathode, as per the reaction $MO_2 + ne^- = M + n/2\ O^{2-}$, where M is the metal. The electrical resistivity of the electro-deoxidation cell will be dependent on (i) transfer of electrons from the lead wire to the oxide pellet, (ii) electrochemical generation of O^{2-} ions at the oxide cathode, (iii) transport of O^{2-} ions from the cathode to the anode through the molten electrolyte medium and (iv) discharge of the O^{2-} ions on the anode to produce CO/CO_2 gas. Steps (i) and (ii) will depend on the electrical characteristics and morphology of the solid cathode whereas (iii) will depend on the diffusion coefficient of oxygen ions in the melt and (iv) on the charge transfer at the reactive anode. At the constant applied current conditions and temperature, steps (iii) and (iv) can be assumed to remain constant. Hence, the changes in the cell resistance during the course of electrolysis can be related to a good extent to the electron transfer reactions taking place at the cathode.

The current versus time plots obtained during constant voltage electro-deoxidation of the TiO_2 and ZrO_2 electrodes, both sintered at 1250 °C, in a two-in-one cell configuration at 3.1 V are given in Fig. 5. The IR drop measurements were carried out at many points during the course of electro-deoxidation. As the current circuit was broken, the current reduced to zero instantaneously, which is seen as the vertical lines in the current–time plots. The corresponding IR drop in the cell voltages was measured

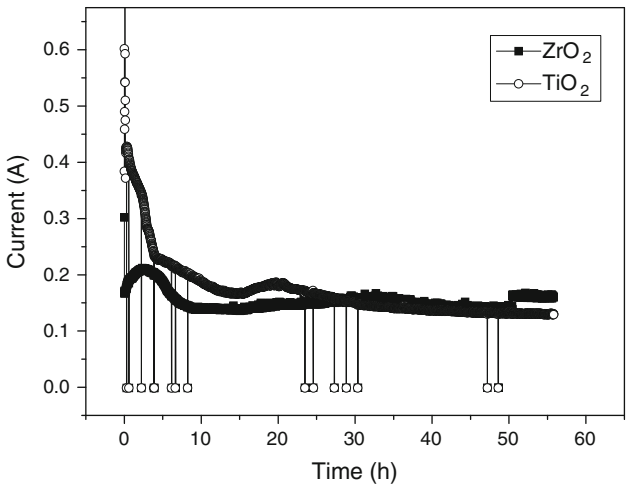

Fig. 5 The current behaviour during constant voltage electrolysis of a two pellets, one ZrO_2 (3.3 mm thick, sintered at 1250 °C for 5 h, open porosity 25.1%) and the other TiO_2 (3 mm thick, sintered at 1250 °C for 2.5 h, open porosity 6.9%), in the two-in-one cell configuration. Applied voltage 3.1 V. The vertical lines are due to the current interruption performed on the cell

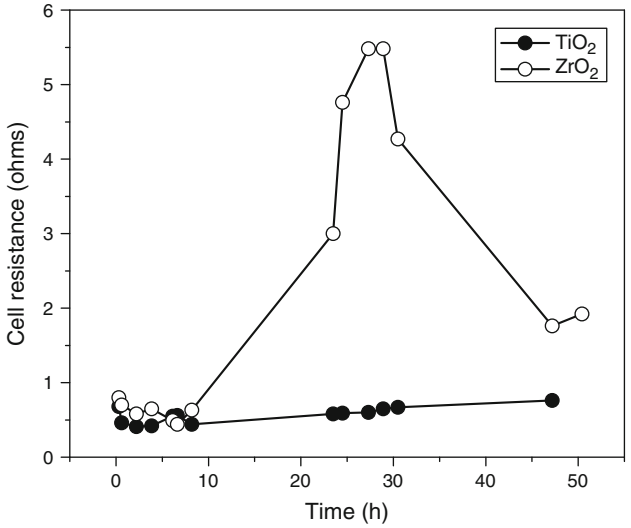

Fig. 6 The resistance of the ZrO_2 and TiO_2 electrodes measured during constant voltage electrolysis (Fig. 5) by the current interruption method. Note that the ZrO_2 electrode became very resistive during electrolysis, whereas the TiO_2 is not

(not shown in the figure), and the cell resistance was calculated from the data as explained in Sect. 2.5.1. The resistance values thus obtained for both the TiO_2 and ZrO_2 cells, are given in Fig. 6. It can be seen from the figure that the resistance of the TiO_2 electrode was not altered much during the course of the electro-deoxidation process, whereas that of the ZrO_2 electrode was increased by a huge factor of over ten in the same period of electro-deoxidation. The cell after attaining the highest resistance of $\sim$5.5 Ω, showed a decreasing trend in resistance with time. Similar results were obtained in an independent experiment with TiO_2 and ZrO_2 electrodes, but electro-deoxidized in the constant current mode. It can be noted from Fig. 6 that the ZrO_2 electrode was highly conducting in the initial stages of electrolysis, turned highly resistive midway through electrolysis and again became conducting towards the end of electro-deoxidation.

A further analysis of the electrolysis curves and the electrical resistivity data is worthwhile in understanding the electro-deoxidation behaviour of the two metal oxides. The electro-deoxidation curves of both the oxides show that the currents are higher in the beginning of the electrolysis, although the currents are substantially higher for titania than zirconia. The flow of high current in the cell, often peaking within a few hours of electrolysis, was reported in many previous electro-deoxidation studies with titanium dioxide and other metal oxides [1, 6, 28]. The low electrode resistance associated with higher currents in the beginning stages of electrolysis would suggest that the starting oxide electrodes behaved as good electronic conductors. Stoichiometric titanium dioxide and zirconium dioxide are known to be insulators. Therefore, the fundamental question arises: how does such an insulating material function as an electrode in an electrochemical cell? This question was answered in many previous studies on the electro-deoxidation of titanium dioxide [1, 5, 6], which invariably suggested that a small amount of oxygen was removed from the stoichiometric pellet at its contact points with the metallic current collector wire, which made the pellet composition non-stoichiometric and hence electronically conducting. If this theory was correct, then it should have taken a while before the whole pellet to become conducting after the initial reactions at the three-phase contact was initiated. Therefore, the peaking of current could have occurred only after this time lag. However, it was noticed in many experiments that a surge of current occurred at the instance of the initial cathodic polarization of the pellet, which indicated that the oxide electrode was indeed a good electronic conductor before it was polarized in the cell. This current surge receded quickly to a more stable value from where it slowly decreased further. This electrode behaviour is evident from the electro-deoxidation curve of TiO_2 given in Fig. 5. It is possible that a small amount of oxygen was lost from the stoichiometric oxide during the high-temperature sintering or while heating it in the experimental vessel under the argon atmosphere at very low oxygen partial pressures and this made the pellet an electronic conductor. The existence of non-stoichiometric and conducting Magnelli phases Ti_nO_{2n-1} ($n = 4$–10) in the Ti–O phase diagram [29] does support this. In the case of ZrO_2, the phase diagram shows the existence of ZrO_{2-x} phase from $\sim$970 °C, though in a very narrow range of x [30]. The sintering of the pellet at

1250 °C and also its long stay in the argon gas environment in the reactor vessel would have given it the small oxygen deficiency to function as an electrode in the cell as experimentally observed. However, the pellet was not expected to show electronic conduction similar to that of TiO_2 pellet and the significantly lower currents of ZrO_2 cathode, seen in Fig. 5 make this fact very clear. The small electronic conductivity acquired by the pellet in the argon gas environment, before its introduction to the melt, would have enhanced further by its immersion in the melt due to the still lower partial pressures of oxygen in the melt. The cathodic reaction also would have helped to enhance the electronic conductivity of the pellet. This aspect will be further discussed in Sect. 3.2.1.

Based on the physico-chemical characterization of the partially reduced samples obtained during the electro deoxidation, Schwandt and Fray [6] reported that the electrochemical reactions taking place on the TiO_2 cathode, in the beginning of electro-deoxidation where higher currents were observed, are essentially the insertion of Ca^{2+} ions on the electrode as

$$5TiO_2 + Ca^{2+} + 2e^- \rightarrow Ti_4O_7 + CaTiO_3 \quad (E^0 \approx +1.807\ V) \tag{1}$$

$$4Ti_4O_7 + Ca^{2+} + 2e^- \rightarrow 5Ti_3O_5 + CaTiO_3 \quad (E^0 \approx +1.678\ V) \tag{2}$$

$$3Ti_3O_5 + Ca^{2+} + 2e^- \rightarrow 4Ti_2O_3 + CaTiO_3 \quad (E^0 \approx +1.575\ V) \tag{3}$$

$$2Ti_2O_3 + Ca^{2+} + 2e^- \rightarrow 3TiO + CaTiO_3 \quad (E^0 \approx +1.200\ V) \tag{4}$$

We have reported similar results on the electro-deoxidation of ZrO_2 pellets with the products of the initial Ca^{2+} insertion reactions being Calcia-Stabilized Zirconia (CSZ), $CaZrO_3$ and Zr, which were transformed to a biphasic mixture of $CaZrO_3$ and Zr at later stages of the electrolysis [20]. The very low resistance of the cathodic reactions of TiO_2, as seen in Fig. 6, suggests that the reactions are quite facile. The positive reduction potentials of the above given equations, support this. Therefore, it can be concluded that the initial reactions can take place rather easily on an oxide electrode polarized cathodically in the molten calcium chloride, provided it is electronically conducting. The ternary compounds formed in this phase of electrolysis will be subsequently decomposed electrochemically to produce the metal–oxygen solid solution, which on continuous electrochemical deoxygenation yields the product metal. The efficiency of the electro-deoxidation reaction will therefore depend a great deal on the electro-deoxidation of the ternary compounds and hence their electronic conductivity. As stated previously, the electro-deoxidation of TiO_2 is reported to proceed via the formation/decomposition of sub-oxides in the sequence, Ti_4O_7, Ti_3O_5, Ti_2O_3 and TiO and ternary compounds $CaTiO_3$ and $CaTi_2O_4$ [6]. The results given in Fig. 6 make it amply clear that all these compounds are good electrical conductors, which helped the electro-deoxidation reaction to proceed without any hindrance. The present experimental results confirm the theory that a metal–oxygen system exhibiting variable metal valence (TiO_2) will show good electronic conductivity, and therefore the direct electro-deoxidation of such metal oxides would be easier than those oxides, which do not satisfy this condition (ZrO_2).

The resistance behaviour of the ZrO_2 electrode clearly establishes that the intermediate compounds formed are resistive in nature, which hinder the reduction process. Analysis of ZrO_2 electrodes, prepared and electro-deoxidized under different experimental conditions, unambiguously confirmed that the pellets were converted to a biphasic mixture of $CaZrO_3$ and Zr, and it was difficult to reduce the electrodes, except under very special conditions [20]. It can be noted from Fig. 6 that the resistance of the ZrO_2 electrode is increasing after ~8 h of electrolysis. The total charge passed during this period was calculated by integrating the area under the *I–t* curve (Fig. 5), and it exceeded the charge necessary for conversion of the whole mass of the pellet (3.83 g) as per the reaction,

$$3ZrO_2 + 2Ca^{2+} + 4e^- \rightarrow 2CaZrO_3 + Zr \quad (E^0 \approx +0.561\ V) \tag{5}$$

by ~20%. Therefore, it can be inferred that the composition of the pellet was changed to $CaZrO_3$. However, it is possible that the charge estimation could be incorrect as secondary reactions are possible in the electro-deoxidation cells. Tien [31] has reported that the progressive addition of CaO to ZrO_2 increased the amount of $CaZrO_3$ in the ZrO_2 phase, which in turn decreased the electrical conductivity. The conductivity decreased sharply at 40 mol% CaO (75 vol.% $CaZrO_3$) as the composition approached the point where the $CaZrO_3$ became the continuous phase. The electrical conductivity decreased to $\sim 10^{-6}\ \Omega^{-1}\ cm^{-1}$ at 900 °C as the composition was changed to $CaZrO_3$. All this information leads us to conclude that the very high resistance of the ZrO_2 electrode, midway in the electro-deoxidation, could be ascribed to the electrochemical formation of the poor conducting $CaZrO_3$ phase. In the absence of variable valence for zirconium, the electrode remained virtually non-conducting at this juncture. However, as can be seen from Fig. 6, the resistance of the electrode decreased as electro-deoxidation was continued. The decrease in the cell resistance can be taken as an indication that $CaZrO_3$ was decomposing as per the reaction,

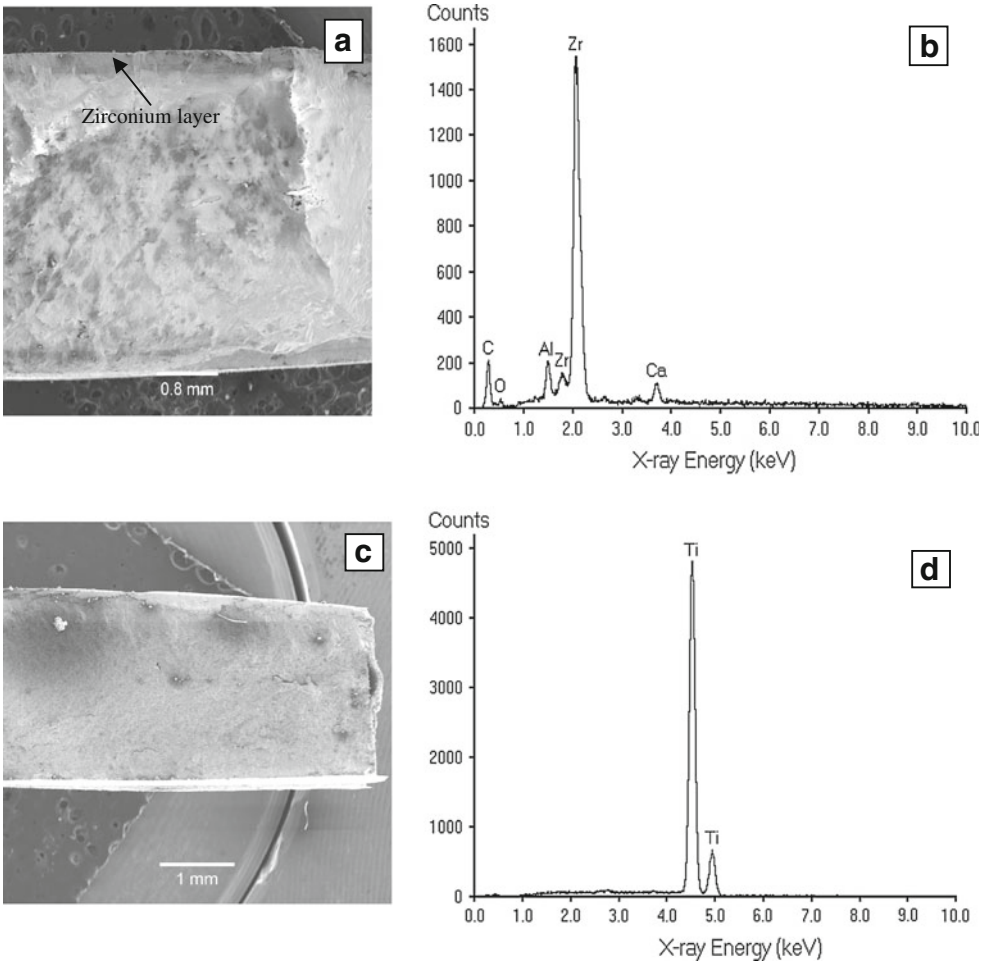

Fig. 7 The scanning electron micrographs of the fractured surface of the **a** ZrO_2 and **c** TiO_2 pellets electrolysed in the two-in-one cell configuration at 3.1 V (Fig. 5). The EDS results obtained from the centre of the surfaces in (**a**) and (**c**) are given in (**b**) and (**d**) respectively. The EDS spectra show an incomplete reduction of ZrO_2 and complete reduction of TiO_2. A thicker layer of zirconium can be seen on the edge of the fractured surface in (**a**)

$$CaZrO_3 + 4e^- \rightarrow Zr + CaO + 2O^{2-} \quad (E^0 \approx +0.286\,V) \qquad (6)$$

As electro-deoxidation continued the zirconium metal layer was formed all along the surface of the pellet, as proposed in the 3DPI mechanism [8], which decreased the electrode resistance further. However, unlike the TiO_2 electrode, the resistance of the ZrO_2 measured towards the end of electro-deoxidation ($\sim$1.8 Ω) is significantly higher than the background level ($\sim$0.5 Ω), and this indicated the presence of insulating compounds in the zirconium metal layer. A physical examination of the sample by SEM showed that this was indeed the case. The bulk of the electrode was only partially electro-deoxidized and contained significant amounts of calcium- and oxygen-containing phases (Fig. 7a, b). About 2 wt% of oxygen was present in the porous metal layer. The distinctly different behaviour of the TiO_2 electrode, depicted in both Figs. 5 and 6, indicated that the electro-deoxidation had proceeded without any hindrance to produce the titanium metal. The results of the SEM/EDAX analysis data given in Fig. 7c, d confirmed this. Using inert gas fusion analysis, it was estimated that the produced titanium metal contained about 5000 ppm of oxygen.

It needs to be mentioned here that complete reduction of ZrO_2 pellets has been reported recently [32], and hence the results discussed in this article may seem to contradict with such results. However, it is clarified that the complete reduction of zirconia pellets was achieved with pellets of thickness 1.5–1.7 mm only, and the inner core of the pellets of >2-mm thickness remained partially reduced only [32]. Electro-deoxidation of the bulk of a ZrO_2 pellet became increasingly difficult as the pellet thickness was increased. The present experiments were carried out with pellets of thickness 3.5 mm and higher, and hence the reduction behaviour was evidently different as explained above.

3.2 Constant current electrolysis

The results of a galvanostatic electro-deoxidation experiment carried out with a TiO_2 pellet (mass 2.353 g, sintered at 1250 for 5 h, open porosity 6.9%) at 100 mA current are given in Fig. 8. A graphite pseudo reference electrode (GRPR) was used to continuously monitor the potential behaviour of both the TiO_2 cathode and graphite anode during the course of the electro-deoxidation experiment.

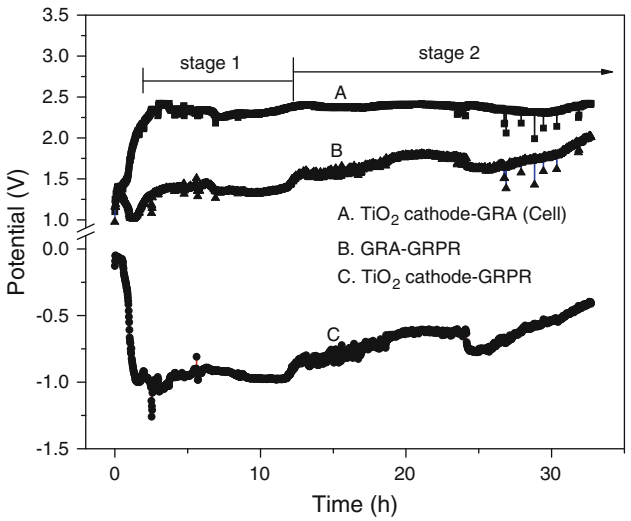

Fig. 8 The potential behaviour of a TiO_2 pellet electrode (3 mm thick, mass 2.353 g, sintered at 1250 for 5 h, open porosity 6.9%) during constant current electrolysis at 100 mA. The *curve A*, *curve B* and *curve C* show the potentials of the electro-deoxidation cell (TiO_2–GRA), the graphite anode versus graphite pseudo reference electrode cell (GRA–GRPR) and the TiO_2 cathode versus graphite pseudo reference electrode cell (TiO_2–GRPR), respectively. Stage 1 and stage 2 marked in the figure refer to the two distinct stages of electrolysis: (1) cathodic insertion of Ca^{2+} ions, and (2) electro-deoxidation of the cathode

The *V–t* curves A, B and C refers to the overall cell voltage of the electro-deoxidation cell (TiO_2–GRA) and the anodic (GRA–GRPR) and cathodic (TiO_2–GRPR) half cell potentials respectively. The electrochemical measurements were made in the DC four contact configuration, as explained in Sect. 2.5.1. The vertical lines dropping from curve A and curve B show the IR voltage drop of the cell A and cell B, respectively, as the current in the electrolysis cell circuit was interrupted. Owing to the low resistance of the titania cathode, the IR drop, though existing, became too small to be visible as a dropping line on curve C.

The cathodic potential can be seen as increasing from the rest potential (30 mV versus the graphite pseudo reference electrode) and more or less stabilizing at ~ -1 V during the beginning 12 h of electrolysis, and thereafter changing slowly in the anodic direction to -0.34 V towards the end of the experiment. Hence, two distinct stages (referred to as stage 1 and stage 2 in Fig. 8) are discernible in the *V–t* plots.

3.2.1 Cathodic potential behaviour

An analysis of the electrochemical behaviour of the cathode, as revealed in the *V–t* curve C, may be possible with a general knowledge of the typical electro-deoxidation behaviour of metal oxides in molten calcium chloride. As mentioned previously, the electro-deoxidation reaction starts with the cathodic insertion of calcium ions from the melt to produce the ternary intermediate compounds, which subsequently decompose and deoxygenate to produce the metal. The cathodic potential measured against a calcium reference electrode will be more positive in the beginning of electro-deoxidation and will become more and more cathodic as the electro-deoxidation continues and finally become close to zero when the oxide electrode has converted to the metal. The cathodic potentials measured by a pseudo reference electrode should also show this decreasing trend, though the absolute values of the measured potentials could be different depending on the difference in the reference potential. This trend is evident in stage 1 of the electro-deoxidation curve C given in Fig. 8. The cathodic potentials measured by the graphite pseudo reference electrode should be related to the oxide ion activity at the cathode, and hence a more or less stable reference cell potential (~ -1 V) recorded in the stage 1 can be taken as a proof that some reactions, which do not alter the oxygen concentration of the cathode in a significant way, are taking place in the region. The calcium insertion reactions (1–4), and the subsequent decomposition reactions of the intermediate compounds as per the reactions

$$2CaTiO_3 + 2e^- \rightarrow CaTi_2O_4 + Ca^{2+} + 2O^{2-} \quad (E^0 > -0.146\ \text{V}) \tag{7}$$

$$CaTi_2O_4 + 2e^- \rightarrow 2TiO + Ca^{2+} + 2O^{2-} \quad (E^0 < +0.417\ \text{V}) \tag{8}$$

can be expected to be occurring in this stage. A steady change of the cathodic potential in the stage 2 may therefore be related to the removal of oxygen from the oxide cathode as per the reaction,

$$TiO + 2(1-\delta)e^- \rightarrow Ti[O]_\delta + (1-\delta)O^{2-} \quad (E^0 \approx +0.177\ \text{V}) \tag{9}$$

If the reaction potentials are considered, then the decomposition reaction (7) cannot be expected to occur in the stage 1, but reaction (8) may be more facile. This may suggest that formation of $CaTi_2O_4$ by the chemical reaction

$$CaTiO_3 + TiO \rightarrow CaTi_2O_4 \tag{10}$$

and its subsequent electrochemical decomposition by reaction (8), as reported by Schwandt and Fray [6], are the two prominent reactions occurring at the cathode. However, it needs to be mentioned that many electrochemical reactions are taking place simultaneously in the solid oxide cathode in the stage 1, which may present mixed potentials of the electrode thus rendering it difficult to identify the different cathodic reactions using the observed electrode potentials alone. Nevertheless, the cathodic potentials and the distinct potential regions indicated in the *V–t* curve are helpful to

monitor the progress of the cathodic process. It should also be mentioned here that, in the present cell configuration, the reference cell and the main cell electrolyte are the same and hence the changes occurring in the chemical composition of the electrolyte melt could influence the reference electrode reactions and hence the reference potentials as explained in Sect. 3.2.3. The systematic variation of the cathodic and anodic potentials in stage 2 (electro-deoxidation region) indicates the changes that are taking place in the chemical composition of the melt with which the pseudo reference electrode is in contact.

The deoxidation experiment was discontinued after 32 h, and the partially electrolysed sample was recovered for analysis. The pellet showed a relatively harder, but friable, crust all along the surface of the pellets and a powdery bulk, which disintegrated during the cleaning process. The XRD spectrum of the crust material (Fig. 9a) shows all the peaks of α-titanium metal (JCPDS: 44-1294), but with the peak positions shifted significantly, suggesting thereby that the material is a solid solution of oxygen in Ti. The bulk material of the pellet (T2) shown in Fig. 9b could not be characterized as it was difficult to completely assign the XRD peaks to any known compounds in the systems Ca–Ti–O or Ti–O, though many peaks matched with those of Ti and $CaTi_2O_4$. SEM pictures of the bulk sample presented a mosaic-like morphology as given in Fig. 9c. These results clearly showed that the electro-deoxidation was incomplete, which indeed should be case as per the *V–t* curves given in Fig. 8.

3.2.2 *Anodic potential behaviour*

The *V–t* curve B in Fig. 8 depicts the electrochemical behaviour of the graphite anode during the electro-deoxidation process. The anodic potential was increased to 1.4 V instantaneously on passing the current (100 mA) through the cell. After remaining a few minutes at 1.4 V, the potential was gradually decreased to ∼0.95 V and thereafter again raised to 1.4 V and maintained there throughout the stage 1 of the electro-deoxidation. Therefore, during stage 1, the overall cell voltage (curve A) can be seen as 2.4 V, the sum of the two half cell voltages.

Two anodic reactions, as given below, are possible in the present electro-deoxidation cell, graphite/$CaCl_2$, CaO/TiO_2.

$$C + O^{2-} \rightarrow CO + 2e^- \quad (E^0 = +1.291\ \text{V}) \tag{11}$$

$$C + 2O^{2-} \rightarrow CO_2 + 4e^- \quad (E^0 = +1.381\ \text{V}) \tag{12}$$

Lebedev et al. [33] reported that the anodic reaction at low current densities is the generation of carbon monoxide. Therefore, it can be reasonably concluded that the

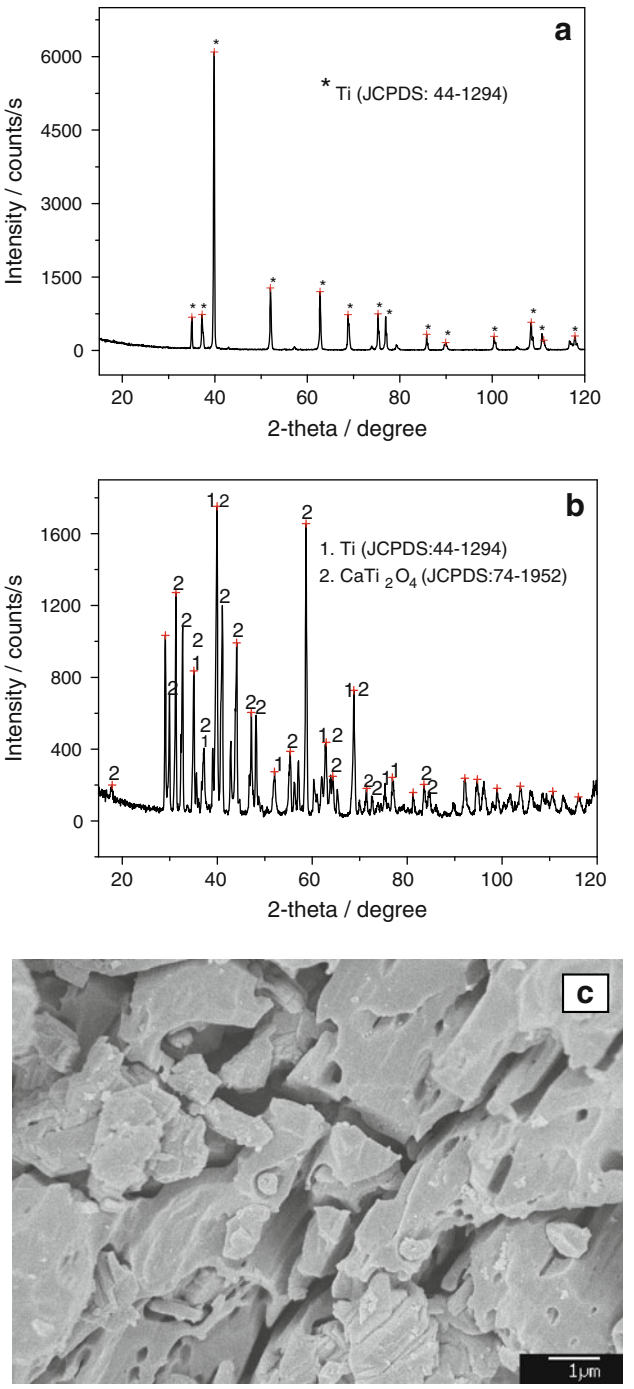

Fig. 9 Results of the XRD/SEM analysis of the TiO_2 pellet, subjected to constant current electrolysis at 100 mA for 34 h (Fig. 7). **a** XRD pattern of the outer crust, **b** XRD pattern of the bulk region and **c** the SEM of the bulk region. The peaks in the XRD spectrum (**a**) match with those of α-Ti metal (JCPDS: 44-1294) but with small deviations in the 2-θ values. The sample is considered as a solid solution of oxygen in titanium. The composition of the bulk part (**b**) could not be determined, as all peaks could not be assigned for any known compound in the system Ca–Ti–O or Ti–O. Many peaks match with those of Ti and $Ca_2Ti_2O_4$ (JCPDS: 11-0029), again with small deviations in the 2-θ values

evolution of carbon monoxide was taking place at the graphite anode in the present cell, except for a short duration of time during which the electrode potential decreased to below 1.4 V. This decrease in the anodic potential from 1.4 to 0.95 V for a short duration of ~1 h in the beginning of electrolysis strongly indicated the presence of an anodic reaction which required less energy than reaction (11), which most probably is the electrochemical adsorption of O^{2-} ions on the active surface sites of the graphite anode as

$$O^{2-} + xC \rightarrow C_xO \text{ (adsorbed)} + 2e^- \quad (13)$$

Mohandas et al. have observed similar electrochemical adsorption of chloride ions on graphite anode in molten sodium chloroaluminate [22]. It was noticed that the chlorine gas evolution on the graphite anode was necessary to activate the electrode for inducing the low energy adsorption/intercalation reaction of chloride ions at the graphite anode. A resistive carbon oxide layer prevented the adsorption of the chloride ions on the fresh graphite anode surface, and the chlorine gas liberating on it probably removed it. In the present case too, such an activation of the graphite anode surface would have been effected by the carbon monoxide liberating on it for a short duration in the beginning of the electrolysis. The retrace of the potential to 1.4 V indicated the reestablishment of electrode reaction (11).

The anodic potential for reaction (11) are related to the activity of O^{2-} ions in the melt as,

$$E = E^0 - RT/2F \ln \text{pCO}/a_{O^{2-}} \quad (14)$$

where E^0 is the standard electrode potential when pCO and $a_{O^{2-}}$ are unity. The partial pressure of the carbon monoxide gas liberated at the anode, under the present experimental conditions, can be considered as unity and therefore any change in the electrode potential is related to the change in the activity of O^{2-} ions in the melt. This would mean that the increase in the anodic potential after the initial dip is indicative of a decreasing O^{2-} ions concentration in the melt due to removal of calcium oxide from the melt. Decomposition of $CaTi_2O_4$ (reaction 8) releases CaO back to the melt and this probably decreased the anodic potentials to below 1.4 V for a duration of about 5 h in the stage 1. Thereafter, the anodic potentials can be seen as increasing continuously. It is possible that the oxygen ions in the melt were depleted during this period. and the electro-deoxidation of the cathode started in the pure calcium chloride melt at ~12 h as per the reaction (9).

3.2.3 *Behaviour of the graphite pseudo reference electrode*

A graphite rod immersed in molten cryolite (Na_3AlF_6) containing dissolved aluminium oxide was reported to give a stable potential for a long duration of time and hence was studied as a pseudo reference electrode in the molten salt system [34]. It is reasoned that the strong adsorption of the oxide ions on the active surface sites of the electrode as per reaction (13) allows an equilibrium

$$CO + 2e \rightleftharpoons C + O^2 \quad (15)$$

to be set up at the electrode–electrolyte interface, whose potential can be represented as

$$E = E^0 - RT/2F \ln a_{O^{2-}}/\text{pCO} \quad (16)$$

where $a_{O^{2-}}$ is the activity of the oxygen ion, pCO is the partial pressure of CO gas and E^0 the standard term in the Nernst equation.

Schwandt et al. [7] and Schwandt and Fray [12] have reported the use of a graphite pseudo reference electrode to monitor/control the half cell potentials during the electro-deoxidation of Cr_2O_3 in molten calcium chloride containing 2 mol% calcium oxide. The concentration of the O^{2-} in the melt was not altered appreciably during electrolysis and hence the electrode potential remained more or less stable throughout the course of the electrolysis. In the present study the pseudo reference electrode was placed in calcium chloride melt to which no CaO was added and hence the graphite reference electrode potential was governed by the small amount of residual CaO (~0.1 mol%) present in the melt. As the CaO concentration in the melt was very low, the potential of the reference electrode became significantly cathodic compared to that of the pseudo reference electrode used by Schwandt and Fray. This was confirmed by cyclic voltammetry measurements, which showed that the calcium deposited at −1.65 V vs the reference electrode as against −1.30 V reported by Schwandt and Fray. As stated previously, most of the oxygen ions in the melt could have been lost towards the end of the electrolysis in stage 1. Under this condition, the deoxidation reaction with a simultaneous build up of calcium, below unit activity, was possible in the melt. This typical electrolyte condition would have made it increasingly difficult for the C/CO equilibrium to be set up in this region and, therefore, most likely, the pseudo reference electrode was changed to an alternate equilibrium

$$Ca^{2+} + 2e^- \rightarrow Ca \quad (17)$$

with the equilibrium potential $E = E^0 - RT/nF \ln a_{Ca}/a_{Ca^{2+}}$, where $a_{Ca^{2+}}$ is a constant and a_{Ca} is a function of the potential at the cathode. Thus, it is considered that the graphite pseudo reference electrode functioned as an O^{2-}-sensing electrode in the pre-electro-deoxidation stage (stage 1) and as a calcium-sensing electrode in the electro-deoxidation stage (stage 2) in the present galvanostatic deoxidation experiment, after being exposed to a low oxygen ion activity and a significant calcium ion activity.

In order to test the hypothesis, a similar electro-deoxidation cell was set up with a new graphite pseudo reference

electrode, whose reference electrolyte was physically separated from the main cell electrolyte, by containing it in a one-end closed high density alumina tube with a very fine orifice at the closed end for electrochemical contact between the two. The reference cell electrolyte contained <0.1 mol% CaO. The half cell potential measurements with the reference electrode showed that the anodic potential remained at 1.5–1.6 V and the cathodic potential at ~ -1.5 V throughout stage 2 of the electro-deoxidation process. This confirmed that the positive deviation of the anodic and cathodic potentials in stage 2 of the galvanostatic experiment under discussion is attributable to the change of the reference electrolyte composition, and hence the transition of the electrode reaction from (15) to (17) as discussed above. The results of the ongoing studies of electro-deoxidation of TiO_2 using the new reference electrode will be discussed in detail elsewhere.

3.2.4 Half cell potentials and electrode overvoltages

If the potential window of a galvanostatic electro-deoxidation experiment is set above the decomposition potential of the calcium chloride electrolyte (3.2 V at 900 °C), then it is possible that the electrolyte will start decomposing at its decomposition potential, once the electro-deoxidation of the electrode is completed. This in other words mean that the calcium metal at unit activity will deposit on the freshly formed metal cathode with simultaneous evolution of chlorine gas on the graphite anode at the end of the electro-deoxidation process. It has been reported in many electro-deoxidation studies that an applied voltage of 3.0 or 3.1 V is necessary for the electro-deoxidation of the metal oxide to the metal of reasonable oxygen purity. Schwandt et al. [7] made detailed study of this aspect and proved that cathodic potentials around calcium deposition are required for the generation of titanium metal of commercially acceptable purity. Our investigation on the electro-reduction of TiO_2 reported in Sect. 2.2 (Fig. 5), also showed that the applied potential has to be 3.1 V or higher to obtain titanium of good purity. Although role of pure metallic calcium in the electro-deoxidation can be ruled out at these applied potentials, the proximity of the applied potential to the decomposition potential of calcium chloride, and hence the cathodic calcium deposition potential is striking. It can be seen from Fig. 8 that the cell voltage (curve A) is remaining stable at 2.4 V for most part of the electro-deoxidation reaction, and it shows an increasing trend towards the end of the experiment. As mentioned above, it is quite clear that the cell voltage would have increased to the decomposition potential of calcium chloride with time, and the cathode would, by then, have been completely deoxidized. This would have meant that the electro-deoxidation in stage 2 was taking place over a potential window in the range of 0 V to 800 mV above the stable potential (2.4 V) of stage 1.

3.3 The current interruption and the potential–time curves

The typical potential–time curves obtained from current interruption of two TiO_2 electro-deoxidation cells, one working at a constant applied voltage of 3.0 V and the other in the constant current mode with 200 mA current, are given in Figs. 10 and 11, respectively. A new graphite pseudo reference electrode, mentioned at end of Sect. 3.2.3, is used in these measurements.

The electrochemical behaviour of the constant voltage cell in the beginning stages of the electro-deoxidation is depicted in Fig. 10. Three current interruptions were made during the period, and the curves show the potential–time profile during the current interruption and current restoration. The three curves denoted by E, A and C in the figure represents the potential–time curves of the overall cell, the anode half-cell and cathode half-cell, respectively. The current is denoted by *I*. The variation of the current and potentials of the cell during electro-deoxidation and while performing the current interruption technique can be traced by following the curves with the alphabets specifically assigned for each channel.

The electro-deoxidation of the second TiO_2 pellet was carried out in the constant current mode for 45 h at

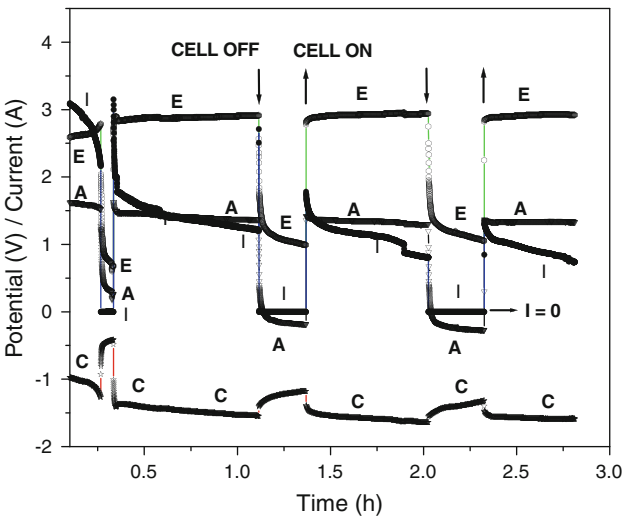

Fig. 10 The variation of current and potential during electro-deoxidation of a TiO_2 cathode in the constant voltage mode at 3 V and while performing the current interruption measurements. Three current interruptions were made on the cell during the beginning 3 h of electro-deoxidation. The *E*, *A* and *C* denotes the overall cell voltage and anode and cathode half cell potentials, respectively. '*I*' represents the cell current. The potential behaviour of the three cells and its course during the current interruption measurements can be traced by following the alphabets *E*, *A* and *C* given near the curves

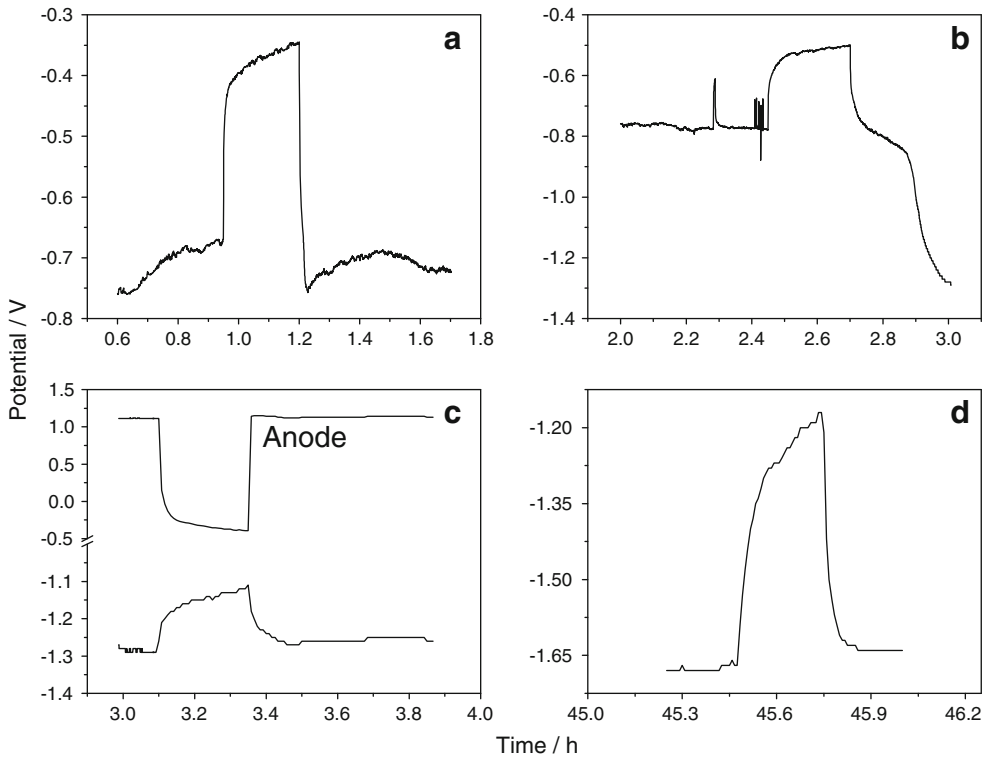

Fig. 11 The cathode potential–time curves obtained during current interruption measurements on an electro-deoxidation cell with TiO_2 cathode and graphite anode. The current interruptions were performed at different times during the deoxidation experiments, as can be seen from the *x*-axis data of the figures. The potential behaviour of the graphite anode during the current interruption is also given in the (**c**). The cathodic potentials were not stabilized in the time interval of the current interruption (15 min), and this indicated that the chemical composition of the electrode was still undergoing change

200 mA current, at the end of which the oxide pellet was converted to titanium metal. Many current interruptions were made at different levels of deoxidation of the pellet by interrupting the cell current for 15 min each time. Typical potential–time curves of the anode and cathode half cells, obtained during the current interruptions, are given in Fig. 11a–d.

Some of the salient features of the potential–time curves are obvious in the *V–t* plots. The anodic and cathodic potentials remained closer in the beginning of the electro-deoxidation and the gap widened as the electrochemical process was continued. In the case of constant voltage cell at 3 V, the cathodic potentials changed rather fast to more cathodic potentials and the potentials remained at −1.5 V and beyond for a significant part of the electro-deoxidation experiment (the cathodic calcium deposition occurred −1.65 V vs the pseudo reference electrode. In the case of the constant current electro-deoxidation cell, the cathodic potentials increased rather slowly and attained the calcium deposition potential in ∼45 h. The *V–t* curve in this case showed some fine features of electro-deoxidation of the solid oxide cathode, which was completely masked in the constant voltage cell (the curves not shown).

It was made clear in the discussions on the novel electrochemical measurements in Sect. 2.5.1 that the reversible decomposition potential (E_{rev}) of an electrode reaction can be obtained from the current interruption measurements (Fig. 4). However, one should be very careful in applying the technique to derive such an equilibrium data of the cathodic reaction of an electro-deoxidation cell. This is so because the current interruption technique described in Sect. 2.5.1 is generally applicable for a stable cell/electrode reaction only, i.e. an electrode reaction where the electrode potential remain constant with time. Electro-deoxidation of an oxide cathode cannot be considered as a stable electrode reaction as the chemical composition of the electrode changes continuously during the electro-reduction process. The *V–t* plot shown in Fig. 11c make this fact amply clear. However, it is possible to fine-tune such experiments to derive critical data of the cathodic process for developing a better understanding of the mechanistic aspects of the electro-deoxidation process. A detailed discussion on such issues of the current-interruption measurements and a finer analysis of the data are not in the scope of this article and those will be presented elsewhere.

3.4 Porosity and mechanical stability of the electro-deoxidized pellets

The resistances of two titania electro-deoxidation cells, one with a titania pellet sintered at 1000 °C, open porosity 40.5% and the other with a pellet sintered at 1250 °C, open porosity 6.9%, measured by current interruption technique during galvanostatic electrolysis at 100 mA current, are given in Fig. 12. It can be seen that except for a few hours in the beginning of electrolysis, the resistance of the cell I is higher than that of cell II throughout the course of the experiment. The result is interesting as it was noticed during electrolysis of TiO_2 pellets, sintered at low temperature (1050 °C or less) that it often resulted in friable product, which crumbled during the cleaning process and its oxygen content was higher, mostly in percentage levels. On the other hand, the electrolysis product of the pellets sintered at higher temperature (1200–1250 °C), could be recovered in a more consolidated form and with a low oxygen content. In fact the TiO_2 pellet used in the experiment described previously in Sect. 3.1 was collected as an excellent titanium metal button with only ~5,000 ppm of oxygen and without any deformation whatsoever, but with a reduction in volume by 22.3% compared to the starting pellet. Therefore, a correlation of the mechanical stability of the electrolysed product and sintering temperature of the starting oxide pellet becomes quite evident.

The major differences between the two titania electrodes can be seen as their extent of porosity and the temperature induced changes in the electrical conductivity. High temperature sintering of a polycrystalline ceramic material makes the smaller grains coalesce and grow in size. As a result the grain boundary resistance for migration of atoms or ions within the solid matrix decreases. In the case of electro-deoxidation, the grain growth of the oxide sample improves the diffusional transport of oxygen in the solid matrix and hence a pellet sintered at a higher temperature can be expected to show lower resistance and also a more efficient removal of oxygen, as revealed in the experiments. The cohesion of the grains achieved in such samples enable the metal grains to be more packed and hence to retain the mechanical integrity of the electrode. Conversely, the deoxidation of the low-temperature sintered (and hence high-porous) pellets, destabilize the cohesion of the product metal grains, which makes the electrode mechanically unstable and the individual grains lose electrical contact. The results underscores the importance of sintering temperature on the electrical conductivity of the electrode, on the stability of the electrode during electrolysis, the feasibility of recovering the metal product in consolidated form and above all the over all electro-deoxidation efficiency. It can be concluded that a metal oxide pellet sintered at a higher temperature would serve as a better electronic conductor and such electrodes could be deoxygenated better. However, good porosity of the electrode is an equally important criterion for the melt to have access to the bulk regions of the solid oxide specimens. Proper design of the oxide electrode, which balances the two important criteria, will be of crucial importance in optimizing the efficiency of electro-deoxidation in the FFC Process.

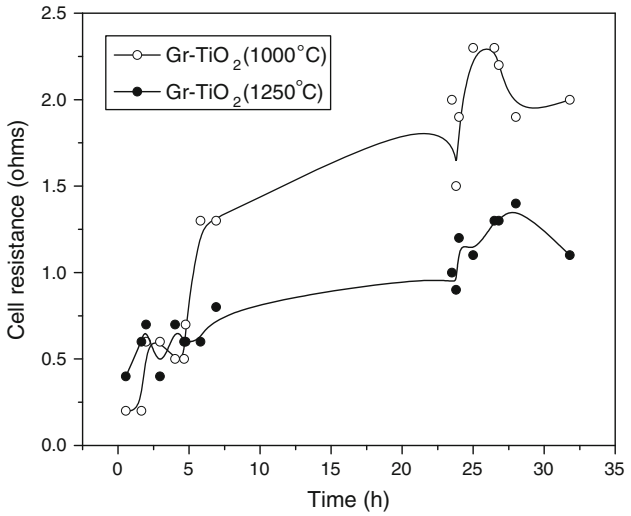

Fig. 12 The variation in the resistances of the two TiO_2 electro-deoxidation cells during galvanostatic electrolysis at 100 mA. The TiO_2 electrodes were sintered at 1000 °C for 3 h (mass 2.397 g, open porosity 40.5%) and 1250 °C for 5 h (mass 2.353 g, open porosity 6.9%). The plots show that the low temperature sintered pellet is more resistive to electro-deoxidation

4 Conclusions

The experimental findings on the electro-deoxidation of titanium dioxide and zirconium dioxide reported in this article, unambiguously demonstrated the capability of the novel electrochemical techniques for study of the fundamental aspects of the complex electro-deoxidation process. These measurements are unique as they are carried out in situ on working cells without causing any disturbance to the experiment and such data are otherwise difficult to obtain from a high-temperature molten salt cell. Such data when used in conjunction with supplementary evidence will help to develop a comprehensive understanding of the electro-deoxidation process.

The cell resistance measurement by the current interruption method, explained and demonstrated in this study, is a simple but potentially useful technique for studying molten salt electrolytic processes. The extension of the technique to measurement of individual electrode resistance, though it needs further development and fine-tuning, is unique as no other techniques are available to obtain the

important information from a working molten salt electrochemical cell. As the cathode resistance is changing continuously, this kind of a measurement will be very useful in the study of the electro-deoxidation process.

The results of the low-current galvanostatic polarization experiment give strong indication that the novel technique can be used effectively for the study of the mechanism of electro-deoxidation process. It needs to be emphasized that just the trend in the electrode potential behaviour and not its absolute values are used in the present analysis because of the inherent limitations of the reference electrode. This is so because the potential of the graphite pseudo reference electrode, when used in the present cell configuration where both the reference and working electrodes are immersed in the same electrolyte, might deviate from its absolute values as the electrolyte composition changes during the long-term electrolysis. Though no significant change in the electrolyte composition is expected in the beginning part of the electrolysis, the electrolyte composition can change with time due to dissolution of the anodic gas and calcium metal and the resulting chemical/electrochemical reactions taking place in the cell.

It is interesting to note that the analysis carried out on the electro-deoxidation of TiO_2 by the new techniques in this article generally agree with those reported by Schwandt and Fray [6] and Schwandt et al. [7] based on the experiments carried out under cathodic potential control and phase analysis of the partially electrolysed samples withdrawn from working cells. The low resistance combined with high currents measured in the beginning of the electrolysis, can be taken as a strong indication that the oxide electrodes were behaving as good electronic conductors from the beginning of electrolysis itself and the electronic conductivity may not be induced by electrode polarization, as reported before. The correlation between the variable valence, electronic conductivity and reduction efficiency of the metal oxide cathode, brought out in this study, is important as it provides an experimental proof to the theory that the metal–oxygen systems with variable metal valence will be good electronic conductors and hence will be more amenable to reduction. The successful reduction of the oxides of Ti, Nb, Ta, and Cr and the relatively poor reduction of the ZrO_2 or Al_2O_3 [35] reported in the FFC process supports this observation.

Overall, the results reported in this study show that the in situ electrochemical measurements are interesting and the new techniques are worth exploring as alternate methods for fundamental studies on the electro-deoxidation process. The techniques need further development and fine-tuning to realize their full potential.

References

1. Chen GZ, Fray DJ, Farthing TW (2000) Nature 407:261
2. Fray DJ, Farthing TW, Chen GZ (1999) International patent no. WO 9,964,638
3. Mohandas KS, Fray DJ (2004) Trans Indian Inst Metals 57:579
4. Rodriguez P, Mohandas KS (2001) Curr Sci 81:443
5. Fray DJ, Chen GZ (2004) Mater Sci Technol 20:295
6. Schwandt C, Fray DJ (2005) Electrochim Acta 51:66
7. Schwandt C, Alexander DTL, Fray DJ (2009) Electrochim Acta 54:3819
8. Chen GZ, Gordo E, Fray DJ (2004) Metall Mater Trans B 35B:223
9. Gordo E, Chen GZ, Fray DJ (2004) Electrochim Acta 49:2195
10. Yan XY, Fray DJ (2002) Metall Mater Trans B 33B:685
11. Yan XY, Fray DJ (2003) J Mater Res 18:346
12. Schwandt C, Fray DJ (2007) Z Naturforsch 62a:655
13. Nohira T, Yasuda K, Ito Y (2003) Nat Mater 2:397
14. Yasuda K, Nohira T, Hagiwara R, Ogata YH (2007) Electrochim Acta 53:106
15. Glowacki BA, Yan X-Y, Fray D, Chen G, Majoros M, Shi Y (2002) Physica C 372–376:1315
16. Wood AJM, Copcutt RC, Chen GZ, Fray DJ (2003) Adv Eng Mater 5:650
17. Bhagat R, Jackson M, Inman D, Dashwood R (2009) J Electrochem Soc 156:E1
18. Örs T, Tan S, Öztürk T, Karakaya I (2009) J Mater Sci 44:3514
19. Zhu Y, Ma M, Wang D, Jiang K, Hu X, Jin X, Chen GZ (2006) Chin Sci Bull 51:2535
20. Mohandas KS, Fray DJ (2009) Metall Mater Trans B 40B:685
21. Mohandas KS (2001) Ph.D Thesis, University of Madras
22. Mohandas KS, Sanil N, Noel M, Rodriguez P (2003) Carbon 41:927
23. Mohandas KS, Sanil N, Mathews T, Rodriguez P (2001) Metall Mater Trans B 32B:669
24. Mohandas KS, Sanil N, Rodriguez P (1998) Curr Sci 75:1166
25. Mohandas KS, Sanil N, Noel M, Rodriguez P (2001) J Appl Electrochem 31:997
26. Mohandas KS, Sanil N, Rodriguez P (2003) Bull Electrochem 19:165
27. Holler FJ, Enke CG (1984) In: Kissinger PT, Heineman WR (eds) Laboratory techniques in electroanalytical chemistry. Marcel Dekker, Inc., New York, pp 241–251
28. Tripathy PK, Gauthier M, Fray DJ (2007) Metall Mater Trans B 38B:893
29. Massalski TB (editor-in-chief) (1990) Binary alloy phase diagrams: Ti-O phase diagram, 2nd edn, vol. 3. ASM International, p 2926
30. Massalski TB (editor-in-chief) (1990) Binary alloy phase diagrams: Zr-O phase diagram, 2nd edn, vol. 3. ASM International, p 2941
31. Tien TY (1964) J Am Ceram Soc 47:430
32. Peng J, Jiang K, Xiao W, Wang D, Jin X, Chen GZ (2008) Chem Mater 20:7274
33. Lebedev VA, Sal'nikov VI, Tarabaev MV, Sizikov IA, Rymkevich DA (2007) Russ J Appl Electrochem 80:1498
34. Minh NQ, Redey L (1987) In: Lovering DG, Gale RJ (eds) Molten salt techniques, Chap. 4, vol 3. Plenum Press, New York, p 105
35. Yan XY, Fray DJ (2009) J Appl Electrochem 39:1349